STM JOURNALS

Journal of
Polymer & Composites

ISSN: 2321-2810 (Online)
ISSN: 2321-8525 (Print)
Volume 14, Special Issue 2, 2026
DOI (Journal): 10.37591/JoPC

https://journals.stmjournals.com/jopc

Research JoPC

Thermal Dissipation Performance of Metal–Polymer Composite Heat Exchanger for Enhanced Thermal Management in Compact Electric Geysers

Neha Dhanawade[1], Shatakshi Joshi[1], Purvi Wankhade[1], Vedant Bhalerao[1], Pramod Kothmire[2]*

Abstract

Most electric geysers these days are made from all-metal stuff, like stainless steel tanks and copper coils for heating, plus mild steel on the outside. Standby heat losses can be 20 to 40 watts, and a 15-litre unit weighs around 6 to 8 kilograms. Manufacturing costs are higher, too. Hard water makes it worse, with limescale building up on the heating elements and cutting thermal conductivity by 10 to 30 percent after a while. This study looks at a new idea, a metal polymer composite for the heat exchanger in a 15 liter domestic geyser. They keep the metal parts for the main heat transfer and to handle pressure, but add polymers like polypropylene, high-density polyethylene, and glass fiber reinforced polypropylene sulfide. These help with better insulation, resisting corrosion, and cutting down the weight overall. For the analysis, they set up equations for heat transfer through the composite walls, hoop stress in the structure, and Nusselt number correlations based on the Dean number for the helical coil. Then they solved them analytically. To check it out, CFD simulations were done with ANSYS Fluent, using a k omega SST model and a mesh of 1.8 million elements. This validated the thermal performance for different configurations. The results show a 31 percent drop in system weight. Standby heat loss goes down to 2.49 watts, which is an 89 percent improvement from the usual 22.4 watts. For the heating cycle, energy use is 193 watt-hours, saving 61 percent compared to traditional ones. The structural part with the SS304 inner tank has a safety factor of 3.22 under pressure, so that holds up fine. Taken all together, this metal polymer setup feels like a solid technical option, and economically, it might make sense for next-generation compact geysers.

Keywords: Metal polymer composite; compact geyser; thermal dissipation; PTC heating element; helical coil heat exchanger; polymer insulation; CFD simulation; standby heat loss; GF-PPS; energy efficiency

INTRODUCTION

***Author for Correspondence**
Pramod Kothmire
ppkothmire@mitaoe.ac.in

[1]UG Scholar, Department of Mechanical Engineering, MIT Academy of Engineering, Pune, Maharashtra, India
2Associate Professor, Department of Mechanical Engineering, MIT Academy of Engineering, Pune, Maharashtra, India

Received Date: April 16, 2026
Accepted Date: April 28, 2026
Published Date: May 08, 2026

Citation: Neha Dhanawade, Shatakshi Joshi, Purvi Wankhade,Vedant Bhalerao, Pramod Kothmire. Thermal Dissipation Performance of Metal–Polymer Composite Heat Exchanger for Enhanced Thermal Management in Compact Electric Geysers. Journal of Polymer & Composites. 2026; 14(Special Issue 2): S618–S651p.

Hot water heating accounts for roughly 18–25% of residential energy consumption in Indian households, placing electric storage water heaters (geysers) among the appliances with the greatest potential for efficiency improvement [1]. With an installed base of over 50 million units growing at 8–10% annually, driven by rapid urbanisation and rising living standards in Tier-2 and Tier-3 cities [2], the scale of the opportunity is hard to overstate. Yet despite decades of growth, the core geyser design has barely changed: a stainless-steel or mild-steel tank, a Nichrome heating coil, polyurethane foam (PUF) insulation, and a mild-steel casing, a combination that continues to produce well-documented thermal inefficiencies.

The most significant limitation is standby heat loss, the energy that leaks away while the geyser sits idle. A standard 15-litre unit with 25 mm of PUF insulation loses 20–40 W continuously, amounting to 0.5–1.0 kWh every day [3]. Over a product lifespan of 5–7 years, this adds up to a substantial economic and environmental burden. A second issue is heating element degradation: in hard-water regions, Nichrome coils accumulate $CaCO_2$ and $MgSO_4$ deposits at a rate of 0.5–2.0 mm per year, progressively cutting heat transfer efficiency by 10–30% and extending heating times [4]. On top of this, the all-metal casing is heavier than it needs to be (6–8 kg) and vulnerable to corrosion in humid environments.

These shortcomings point naturally toward hybrid material architectures, designs that use metals where their strength and conductivity matter, and polymers where insulation, corrosion resistance, and weight savings are the priority. This role-specialization principle has been well validated in industrial heat exchangers [5,6], but remains largely unexplored in the context of domestic geysers. Candidate polymers for this application include polypropylene (PP), high-density polyethylene (HDPE), and glass-fibre reinforced polyphenylene sulphide (GF-PPS), all of which offer low thermal conductivity and sufficient temperature resistance for continuous hot-water service (100–220°C) [7, 8].

When combined with a PTC ceramic heating element and a helical copper coil that boosts heat transfer through Dean vortex action, along with a dual-layer PUF + Vacuum Insulation Panel (VIP) arrangement, the resulting system significantly outperforms conventional designs.

Against this backdrop, the present study investigates a metal–polymer composite heat exchanger for a 15-litre geyser. The work covers: (i) thermal and structural modelling; (ii) CFD validation using ANSYS Fluent (k–ω SST model); (iii) performance comparison with conventional designs; and (iv) identification of the optimal polymer configuration for the Indian market.

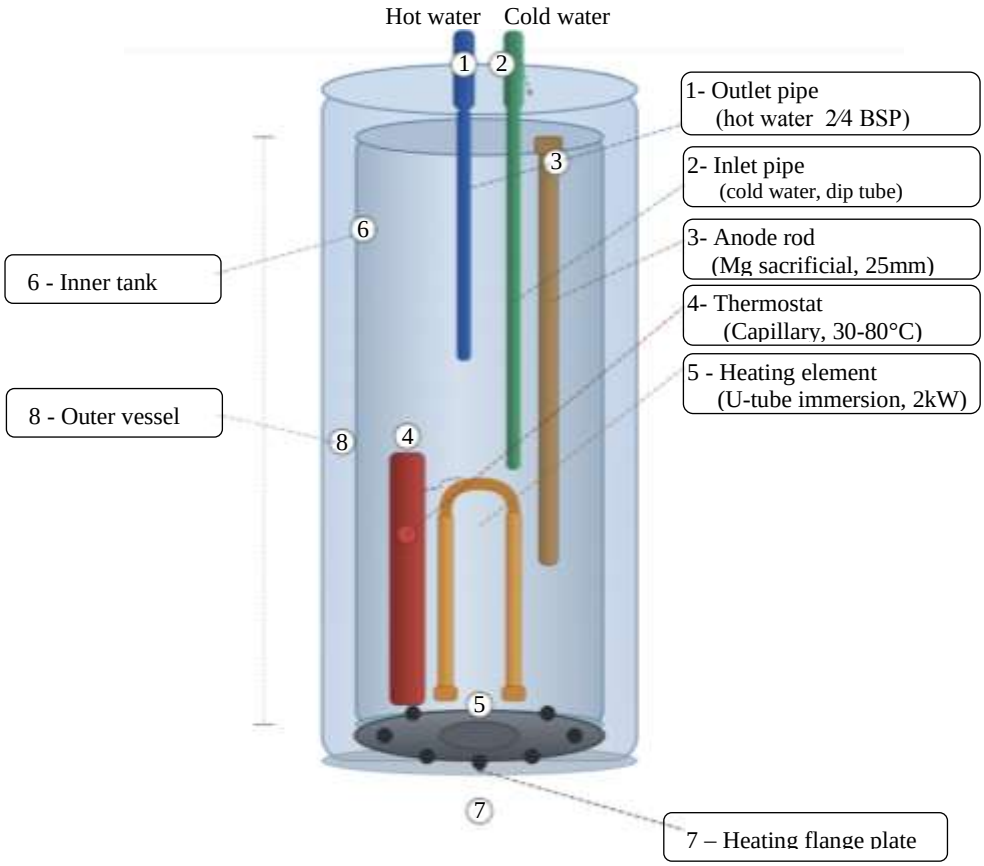

Figure 1. Schematic diagram of an electric storage water heater (geyser) illustrating key internal components.

LITERATURE SURVEY

Research on domestic electric water heaters has evolved considerably over the past two decades, progressing from studies of basic storage-tank behaviour toward increasingly sophisticated material, geometric, and control-based optimisation strategies. The Bureau of Energy Efficiency, India (2023) [1] documented that electric water heaters account for a disproportionate share of residential electricity consumption, making them one of the highest-impact appliances for efficiency intervention. The CEAMA-Frost and Sullivan report (2022) [2] established the market scale, recording an installed base exceeding 50 million units in India, growing at 8 to 10 percent annually due to rapid urbanisation and rising living standards in Tier-2 and Tier-3 cities. Singh and Mehta (2022) [3] characterised standby energy losses in residential electric water heaters in detail, quantifying the 20 to 40 W continuous loss range that makes idle operation the dominant source of inefficiency over a product's service life. Prakash and Jain (2021) [4] quantified heating element degradation under hard-water conditions, showing that limescale deposition on Nichrome coils at a rate of 0.5 to 2.0 mm per year reduces heat transfer efficiency by 10 to 30 percent and progressively extends heating times, establishing the technical case for alternative heating element materials and surface-resistant designs. The use of polymers in heat exchanger design has been a subject of sustained research. Zaheed and Jachuck (2004) [5] provided a foundational review of polymer compact heat exchangers, highlighting their corrosion resistance, low fouling tendency, and suitability for aggressive fluid environments. Cevallos et al. (2012) [6] surveyed the historical development and remaining engineering challenges of polymer heat exchangers across industrial sectors. Wypych (2019) [7] and Ebnesajjad (2018) [8] provide authoritative material property data for engineering thermoplastics including polypropylene, HDPE, and glass-fibre reinforced polyphenylene sulphide (GF-PPS), confirming continuous use temperatures of 100 to 220 degrees Celsius and low thermal conductivities of 0.19 to 0.35 W/m.K. Broniarz-Press et al. (2007) [9] confirmed the heat transfer performance of polymer composite materials in heat exchanger applications, and Zaheed and Jachuck (2004) [10] demonstrated the viability of a square cross-corrugated polymer film heat exchanger in compact configurations. Huang et al. (2023) [11] developed thermal resistance models for polymer-coated metallic pressure vessels in hot-water contact, directly relevant to composite geyser wall analysis. Akcay and Sayman (2001) [12] investigated burst pressures of composite cylinders under internal pressure, informing the structural safety analysis of composite wall designs. Chen et al. (2016) [13] provided a comprehensive review of recent developments in polymer heat exchangers covering material selection, fouling behaviour, and pressure resistance. Bahrami et al. (2004) [14] addressed thermal contact resistance at polymer-metal interfaces, a critical parameter in composite wall heat transfer calculations. Celen et al. (2025) [15] reviewed recent advancements in polymer heat exchanger technology with specific attention to heat transfer performance improvements. Deka et al. (2022) [16] confirmed long-term material reliability through a hydrothermal ageing study of GF-PPS composites, showing acceptable property retention after prolonged immersion at elevated temperatures, validating GF-PPS as a candidate material for continuous hot-water service. Bigg (1986) [17] established early foundational data on thermally conductive polymer compositions. Dreiser and Bart (2014) [18] specifically addressed mineral scale control in polymer film heat exchangers, confirming that polymer surfaces resist the CaCO3 deposition that degrades Nichrome heating elements in hard-water conditions. Kaushik and Ranjan (2021) [19] reviewed the cost-performance suitability of polymer composite materials for domestic appliance casings in the Indian market, confirming economic viability for mass-market applications. Torres-Martinez et al. (2025) [20] demonstrated a solar water heater incorporating polypropylene nanocomposites, confirming the broader applicability of polymer-based composite structures in domestic thermal appliance contexts.

Hollow-fibre polymer heat exchanger configurations were explored by Sirkar (2010) [21] and Astrouski et al. (2015) [22], demonstrating compact, high-surface-area designs with strong fouling resistance in thermal desalination and automotive radiator applications, respectively. Meyers et al. (2003) [23] demonstrated through national policy analysis that energy efficiency standards for residential water heaters deliver substantial electricity savings at scale, reinforcing the policy relevance of improved geyser design. Brunner and Simmler (2008) [24] assessed Vacuum Insulation Panels (VIP)

in situ, showing thermal conductivities as low as 0.004 W/m.K, far superior to conventional polyurethane foam insulation for standby heat retention. Li et al. (2020) [25] characterised self-regulating PTC barium titanate ceramic heating elements and confirmed their suitability for domestic water heater applications, where self-limiting behaviour eliminates overheating risk. Chen et al. (2019) [26] showed that demand-responsive smart thermostat algorithms reduce water heater electricity consumption by 15 to 20 percent without any hardware modification, establishing the value of intelligent control as a complementary efficiency measure. Siddiqui et al. (2021) [27] compared rectangular and cylindrical pressure vessel geometries through finite element analysis, providing structural insight relevant to tank geometry selection. Jayakumar et al. (2008) [28] conducted experimental and CFD-based estimation of heat transfer in helically coiled heat exchangers, deriving validated Dean number-based Nusselt number correlations that remain widely cited in coil design. Kharat et al. (2009) [29] developed heat transfer coefficient correlations specifically for concentric helical coil heat exchangers, capturing the geometric dependency used in the present coil optimisation. Consul et al. (2004) [30] developed a combined fluid dynamics and heat transfer numerical methodology for virtual prototyping of storage-type domestic hot-water heaters, providing the CFD framework foundation for subsequent studies, including the present work. The Bureau of Energy Efficiency (2022) [31] set the regulatory baseline through energy conservation and star-rating standards for electric water heaters in India. Pathak et al. (2022) [32] used CFD to study the effect of inlet velocity on thermal stratification in helical coil water heater tanks, confirming the importance of flow regime in heating efficiency. Pal et al. (2016) [33] examined the influence of baffle inclination on shell-and-tube heat exchanger performance, providing experimental benchmarks for CFD validation. Pawar and Sunnapwar (2013) [34] conducted experimental heat transfer studies in helical coils across laminar and turbulent regimes for Newtonian and non-Newtonian fluids, offering empirical data directly applicable to helical coil geyser designs.

Complementary CFD and experimental investigations by research groups at the authors' institution have built a substantial knowledge base directly relevant to compact heat exchanger and geyser design. Damdhar et al. (2022) [35] analysed exhaust gas flow through mufflers using CFD, validating the pressure-loss prediction capability of the numerical framework applied here. Deshmukh et al. (2023) [36] conducted experimental heat transfer studies in composite vessels, directly informing the composite wall thermal analysis of the proposed geyser design. Gadave and Kothmire (2019) [37] evaluated the thermo-hydraulic performance of shell-and-tube heat exchangers across varying tube geometries, establishing the strong geometric dependence of heat transfer enhancement. Kanate et al. (2022) [38] investigated CPU heat sink performance numerically, reinforcing best practices in meshing and boundary condition setup for compact thermal devices. Kumavat and Kothmire (2023) [39] performed CFD and experimental analysis for optimal cooling system design in theatres, validating the k-omega SST turbulence model for enclosed thermal environments. Londhe et al. (2023) [40] studied the impact of economiser tube geometry on water heating performance, providing directly relevant insight into coil geometry effects on heating efficiency. Narad et al. (2022) [41] numerically investigated the effective positioning of air conditioning units in office rooms, further validating the CFD methodology used. Nagarhalli et al. (2023) [42] studied natural and forced convective heat transfer from finned spheres, demonstrating the performance gains achievable through geometry-based enhancement. Nawale et al. (2021) [43] showed that twisted tape inserts in heat exchangers produce significant heat transfer enhancement, relevant to internal coil surface treatment. Pawar et al. (2022) [44] performed CFD analysis of different greenhouse designs, adding further breadth to the validated CFD portfolio. Powar et al. (2022) [45] examined the effect of surface roughness on boundary layer thickness, with implications for wall heat transfer modelling in composite geyser systems. Shindge et al. (2022) [46] used CFD to optimise back pressure and velocity in a catalytic converter, confirming the framework's capability for complex internal flow problems. Tajane et al. (2023) [47] investigated radiative heat transfer for room cooling through both experimental and CFD methods, broadening the thermal modelling validation base. Yadav and Kothmire (2021) [48] performed CFD analysis of a diesel engine exhaust pipe, further establishing the reliability of the CFD approach for thermal flow problems relevant to the present study.

Taken together, this body of literature covers significant ground: energy policy and market context, standby loss characterisation, polymer material properties and durability, heat exchanger design and coil correlations, structural analysis of composite pressure vessels, CFD methodology validation, and heat transfer enhancement techniques. However, the synthesis of all these elements into a single integrated compact geyser design remains largely unaddressed. No published study has simultaneously combined a metal-polymer composite wall architecture, VIP-enhanced insulation, a PTC heating element, a Dean-vortex helical coil, and intelligent control within one system and evaluated the combined performance benefit analytically and computationally. This gap is the direct motivation for the present work.

RESEARCH GAPS

Integrated Performance Optimisation

The bulk of existing work addresses individual improvements in isolation, whether a better heat transfer coefficient, an improved insulation layer, or a modified heating mechanism, without considering how these parameters interact in practice. Real geyser performance, however, depends on exactly those interactions. A design framework that simultaneously optimises heating time, thermal efficiency, and compactness is conspicuously absent from the literature. Without this, gains in one area frequently come at the expense of another, capping the overall benefit.

Energy Efficiency and Power Consumption

Technologies like PTC heating elements and advanced insulation have each demonstrated energy-saving potential individually, but their combined deployment within a single system remains rare. More importantly, most studies stop short of addressing how power consumption should be managed dynamically under real operating conditions. Without real-time control strategies such as adaptive power regulation, temperature feedback, and demand-responsive heating, energy utilisation remains suboptimal, and electricity consumption stays higher than it needs to be.

Material Integration and Smart Control Systems

Polymers, vacuum insulation panels (VIP), and composite structures each bring clear benefits, including better thermal insulation, corrosion resistance, and reduced weight, but the question of how to integrate them effectively with intelligent control systems has not been seriously tackled. The particular combination of metal-polymer composite construction with smart sensors and automated control remains underdeveloped, and this limits how much performance and operational efficiency can realistically be extracted from compact geyser designs.

Geometric Optimisation and Weight Reduction

Most conventional geysers rely on cylindrical geometries by default, even though these are not always the best choice in terms of surface-area-to-volume ratio or heat retention. Alternative geometries that could improve thermal performance while reducing physical size remain largely unexplored. The weight reduction potential of polymer-based and hybrid materials has similarly gone under-utilised, leaving current designs bulkier than necessary for the space-constrained homes that increasingly characterise urban India.

OBJECTIVES AND SCOPE

This section presents a detailed analysis of the performance of the proposed metal–polymer composite geyser design using both analytical methods and CFD simulations. The results focus on key performance indicators, including heat transfer enhancement, standby heat loss reduction, structural safety, and overall system efficiency. Initially, the effect of Dean vortex–induced mixing in the helical coil is validated, followed by a comparative evaluation of multiple design configurations with varying insulation and casing materials. The role of polymer integration is examined in terms of its contribution to thermal resistance, weight reduction, and cost effectiveness. Structural integrity of the hybrid configuration is also assessed to ensure safe operation. The discussion further highlights the combined

influence of improved heating mechanisms, advanced insulation, and optimised design on energy consumption, heating time, and suitability for compact domestic applications.

Reduction in Heating Time

A central aim of this work is to cut the heating time of compact domestic geysers by improving heat transfer efficiency and refining the heating mechanism. Through the use of advanced heating technologies and more effective heat exchange methods, the system is designed to achieve a faster temperature rise, reducing how long users have to wait and making the geyser more responsive in everyday use.

Minimisation of Power Consumption

Reducing electricity consumption is equally important. The study pursues this through energy-efficient components and intelligent control strategies, in particular PTC heating elements, which self-regulate their power output, combined with variable power control and sensor-based automation. Together, these measures ensure the system draws only the energy it actually needs, avoiding unnecessary consumption and improving overall efficiency.

Improvement in Thermal Efficiency and Heat Retention

The study also targets improved thermal efficiency by tackling heat loss during both active heating and standby periods. Advanced insulation materials, notably Vacuum Insulation Panels (VIP), are incorporated to slow heat escape and support thermal energy retention. The practical effect is that water stays hot for longer, reducing how often the heating element needs to cycle back on.

Development of Compact and Lightweight Design

Finally, the design aims to be genuinely compact and lightweight, practical for the kinds of space-constrained homes that are increasingly common in urban India. This means optimising tank geometry and the volume-to-surface-area ratio to minimise heat loss without sacrificing storage capacity, while also keeping material use and therefore weight as low as possible. The result is a design that is easier to install and handle without any trade-off in performance.

METHODOLOGY

To establish a robust evaluation framework, the study first focuses on the development of a three-dimensional computational model that represents the primary components of the compact electric geyser, including the inner storage tank, helical copper heating coil, and outer casing. Various design configurations were created by systematically varying the insulation layers, such as PUF and VIP, and the casing materials, including metal and polymer composites like GF-PPS, PEEK, and PP. The geometry for each scenario was meticulously designed to maintain a constant storage capacity of 15 litres, ensuring a controlled environment for a comparative analysis of different structural arrangements and their impact on thermal performance.

Geometry Development

A three-dimensional model of the compact electric geyser was developed to represent the inner storage tank, helical copper heating coil, and outer casing as shown in the Figure 1. Multiple design configurations were created by varying insulation layers (PUF, VIP) and casing materials (metal and polymer composites such as GF-PPS, PEEK, and PP). The geometry was designed to maintain a constant storage capacity of 15 litres while enabling comparative analysis across different structural arrangements.

CFD Analysis

Three-dimensional CFD simulations were performed in the ANSYS FLUENT solver to validate the analytical model predictions and characterise tank-wide temperature distribution. All CFD simulations presented in this study were carried out using the ANSYS Fluent software platform accessed through a

valid institutional research licence during the execution of the project.The computational domain included the helical copper coil (15 mm OD, 8 turns, 20 mm pitch, 190 mm centreline diameter).

Fluid Flow Analysis

The fluid flow analysis of the helical coil heat exchanger was carried out using ANSYS Fluent 2026 R1. The simulation aimed to study the internal flow behaviour, velocity distribution, and pressure drop characteristics of the fluid flowing through the helical coil geometry under defined boundary conditions.

Geometry

The three-dimensional geometry of the helical coil was modelled in ANSYS Design Modeler. The model represents a helical coiled tube configuration wound in a cylindrical arrangement, consisting of multiple turns with a straight inlet and outlet section extending vertically from the coil. The coil spans approximately 190 mm in the axial direction, as indicated by the scale bar in the geometry view. The helical tube has a circular cross-section and is designed to simulate the internal fluid domain through which the working fluid flows. The geometry captures the continuous curvature of the helical path, which is known to induce secondary flow effects (Dean vortices) that enhance heat transfer and mixing within the tube. The 3D model, as generated in Fusion 360, is shown in Figure 2.

Meshing

The computational domain was discretised using an unstructured tetrahedral mesh generated in ANSYS Meshing 2026 R1 as shown in the Figure 3 and presented in Table 1. The meshing algorithm automatically conformed to the complex helical curvature of the geometry, producing a fine, densely packed triangular surface mesh with tetrahedral volume elements throughout the fluid domain. Inflation layers were applied near the tube wall surfaces to accurately resolve the boundary layer and near-wall flow gradients, which are essential for turbulent flow simulations.

Figure 2. Three-dimensional CAD geometry of the helical coil heat exchanger modelled in ANSYS Design Modeler 2026 R1, showing the continuous helical tube configuration with vertically extended straight inlet and outlet sections. The coil spans approximately 200 mm in the axial direction with a circular cross-sectional tube profile wound in a cylindrical arrangement.

Table 1. Computational mesh details showing unstructured tetrahedral discretisation and mesh parameters used for accurate CFD analysis.

Mesh Parameter	Value
Mesh Type	Unstructured tetrahedral

Nodes	309255
Elements	1180515

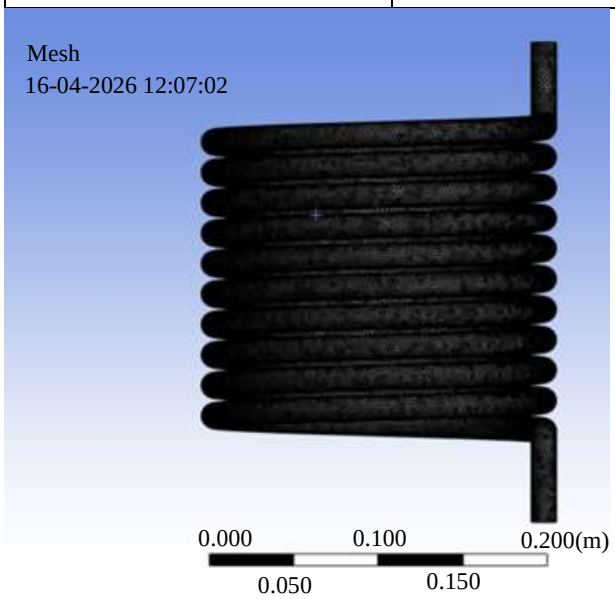

Figure 3. Unstructured tetrahedral mesh generated on the helical coil fluid domain in ANSYS Meshing 2026 R1 (16-04-2026), showing the densely packed triangular surface elements conforming to the complex helical curvature. Inflation layers are applied along the tube wall surfaces to accurately resolve near-wall boundary layer gradients essential for turbulent flow simulation.

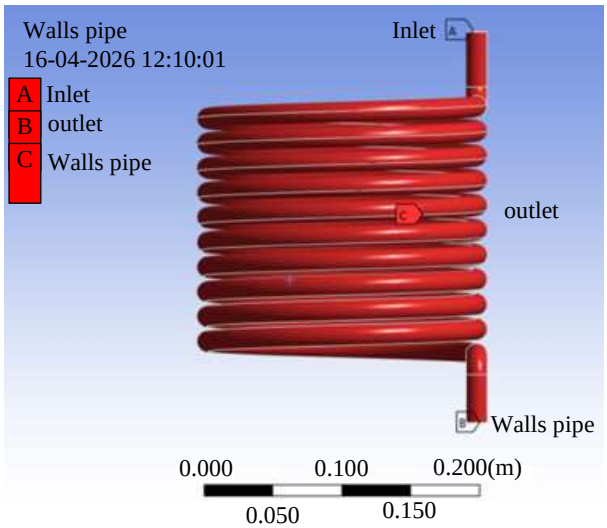

Figure 4. Named selection assignments defined on the helical coil geometry in ANSYS Fluent 2026 R1 (16-04-2026), identifying three boundary zones — (A) Inlet: the top face of the inlet pipe where fluid enters at 1.5 m/s; (B) Outlet: the bottom face of the outlet pipe set to zero gauge pressure; and (C) Walls Pipe: the entire inner helical tube surface defined as a no-slip wall boundary condition.

The mesh density is higher along the curved sections of the helical coil to capture the flow curvature effects accurately.

Name Selection

To apply boundary conditions precisely, named selections were defined on the relevant faces of the geometry in ANSYS Meshing as shown in the Figure 4. Three named selections were assigned as follows:

These named selections ensured that boundary conditions were applied accurately during the solver setup in ANSYS Fluent.

Table 2. Boundary Conditions and solution methodology used in ANSYS Fluent for simulating the thermal dissipation performance.

Parameter	Value/Setting
Solver Type	Pressure-Based, Steady State
Turbulence Model	k- ω SST (Shear Stress Transport)
Fluid	Water (liquid)
Inlet Boundary	Velocity Inlet- 1.5 m/s
Outlet Boundary	Pressure Outlet – 0 Pa (gauge)
Wall Condition	No slip Condition
Solution Method	Simple Algorithm

Table 3. Engineering polymer comparative property matrix for outer casing selection (GF-PPS selected as primary recommendation)

Property	GF-PPS	PEEK	PP	HDPE	SS304 (ref.)
Cont. use temp. (°C)	220	250	100	80	870
Tensile strength (MPa)	120–180	100–200	25–40	20–30	515
Thermal conductivity (W/m·K)	0.28	0.25	0.22	0.44	16.0
Density (g/cm³)	1.60	1.32	0.91	0.95	7.93
Hot-water resistance (80°C)	Excellent	Excellent	Good	Good	Good (coated)
Cost vs SS304 baseline	−22%	+15%	−35%	−40%	Baseline

Boundary Conditions

The simulation was set up in ANSYS Fluent using the following boundary conditions and solver settings as presented in Table 2.

The k-ω SST turbulence model was selected due to its superior performance in predicting turbulent flows in curved geometries. It combines the robustness of the k-ω model near the wall with the accuracy of the k-ε model in the free-stream region, making it the most suitable model for internal helical pipe flows where adverse pressure gradients and secondary flows are present. The simulation was run for a maximum of 1000 iterations. The solution achieved convergence at approximately 600 iterations, where all residuals, including continuity, momentum (x, y, z), turbulent kinetic energy (k), and specific dissipation rate (ω) dropped below the convergence criterion of 1×10^{-3}. This indicates a stable and physically consistent flow solution was obtained well within the iteration limit.

Governing Equations

The flow and heat transfer inside the geyser were modeled using the fundamental conservation equations.

Continuity Equation (Mass Conservation):

$$\nabla \cdot (\rho \vec{V}) = 0$$

Momentum Equation (Navier–Stokes):

$$\rho(\vec{V} \cdot \nabla)\vec{V} = -\nabla P + \mu \nabla^2 \vec{V}$$

Energy Equation:

$$\rho c_p(\vec{V} \cdot \nabla T) = k\nabla^2 T$$

These equations were solved under steady-state conditions using appropriate boundary conditions for heat flux, inlet temperature, and wall interactions.

Polymer Material Selection

Three polymer grades were evaluated for the outer casing application against five weighted criteria: continuous use temperature (≥ 80°C required), tensile strength (≥ 80 MPa), thermal conductivity (≤ 0.35 W/m·K), hot-water chemical resistance, and unit cost relative to the SS304 outer casing baseline. Table 3 presents the comparative property matrix.

RESULTS & DISCUSSION

The velocity streamline plot (Figure 5) illustrates the path taken by fluid particles as they travel through the helical coil from inlet to outlet. The streamlines are colour-coded by velocity magnitude, ranging from a minimum of 0.1845 m/s to a maximum of 2.177 m/s. The fluid enters at the top inlet pipe and immediately follows the helical path. Higher velocities (shown in red and orange) are observed along the inner radius of each coil turn, while lower velocities (shown in blue and green) appear near the outer walls. This asymmetric velocity distribution is characteristic of Dean flow, the secondary circulatory motion induced by centrifugal forces in curved pipes, which plays a significant role in enhancing the convective heat transfer within helical coils.

The cross-sectional velocity contour plots (Figure 6) depict the velocity distribution across the tube cross-section at multiple locations along the coil. The velocity ranges from 0.1845 m/s to 2.177 m/s, with the peak velocity concentrated towards the inner (upper) portion of the cross-section. The outer wall region exhibits lower velocities due to the centrifugal effect pushing the high-momentum fluid toward the inner curvature. This skewed velocity profile deviates from the parabolic distribution observed in straight pipe flow and is a direct consequence of the helical curvature. The Dean vortex pairs visible in the contour cross-sections confirm the presence of secondary flow structures that promote fluid mixing and enhance thermal performance.

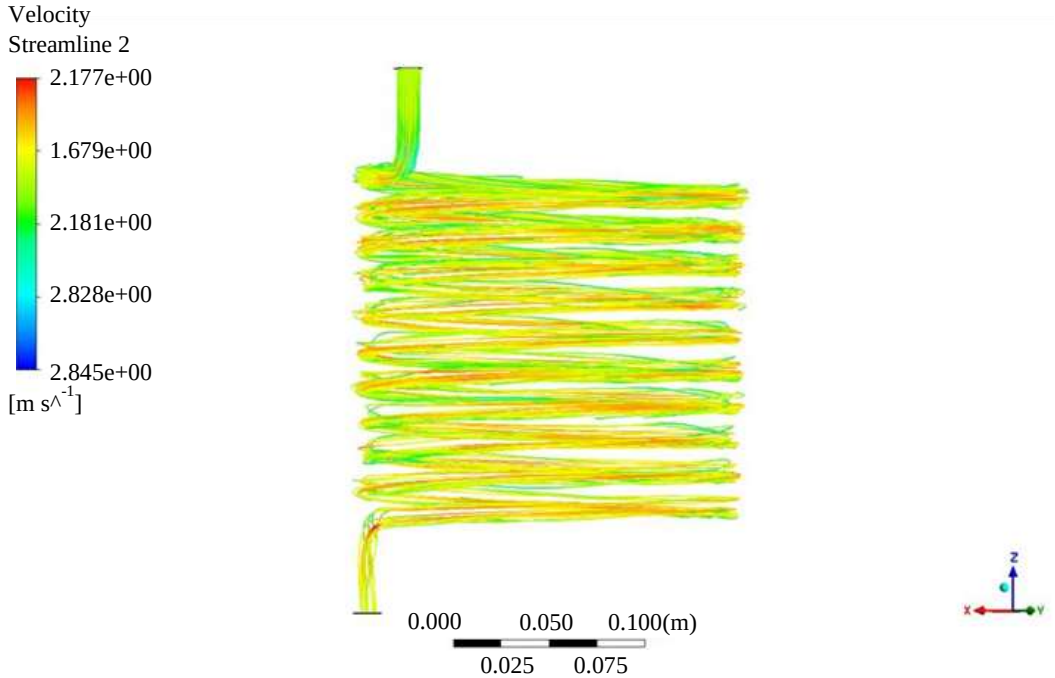

Figure 5. Velocity streamline plot of the fluid flow through the helical coil heat exchanger obtained from ANSYS Fluent simulation, colour-coded by velocity magnitude ranging from 0.1845 m/s (blue) to 2.177 m/s (red). The streamlines trace the helical path of fluid particles from the top inlet to the bottom outlet, revealing higher velocities concentrated along the inner radius of the coil bends and lower velocities near the outer wall. This asymmetric velocity distribution confirms the presence of Dean

flow, centrifugally induced secondary circulation characteristic of turbulent flow in curved pipe geometries.

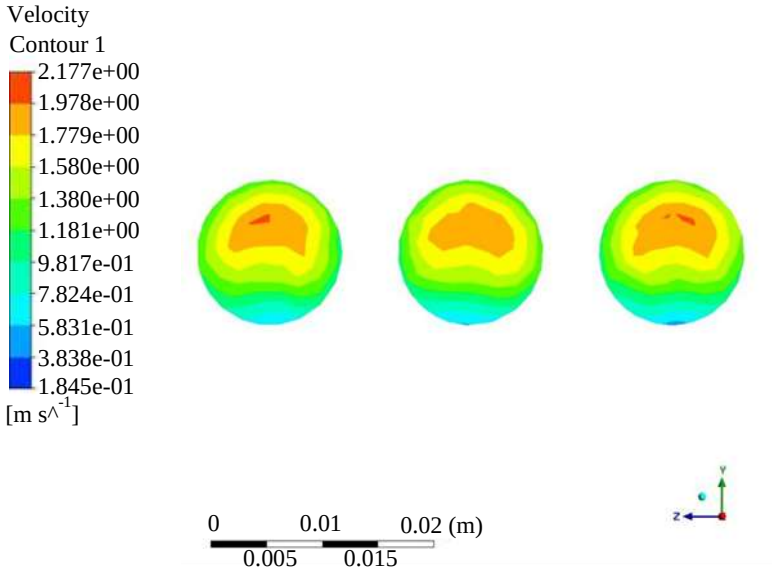

Figure 6. Cross-sectional velocity contour (Contour 1) at three representative locations along the helical coil tube, obtained from ANSYS Fluent simulation. The velocity magnitude ranges from 0.1845 m/s (blue, near outer wall) to 2.177 m/s (red, inner region), illustrating the skewed and asymmetric velocity profile induced by the helical curvature. The concentration of peak velocity toward the inner curvature of the tube cross-section confirms the centrifugal effect and the development of Dean vortex pairs, which deviate significantly from the parabolic profile observed in straight pipe flows.

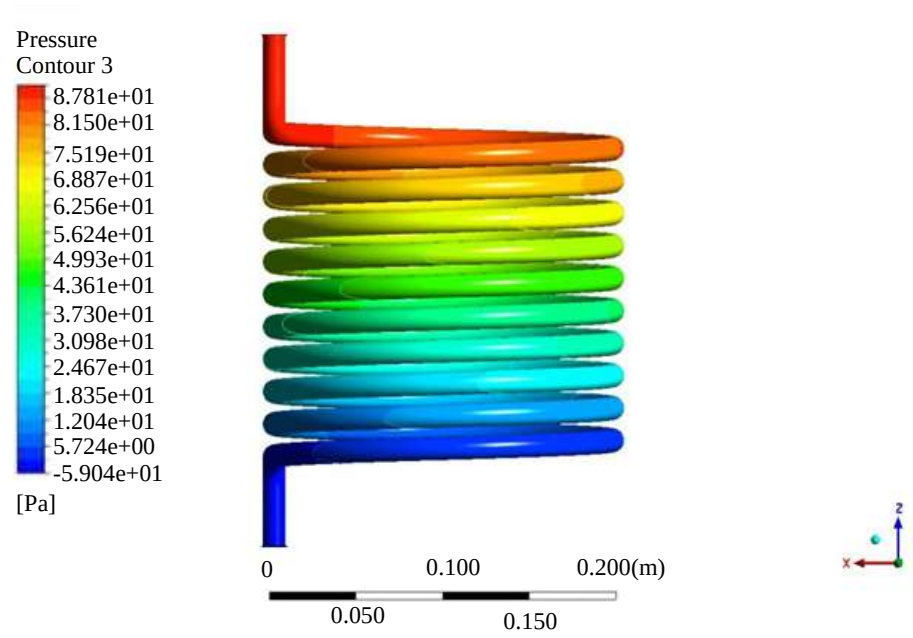

Figure 7. Static pressure contour of the helical coil heat exchanger obtained from ANSYS Fluent simulation, displaying the pressure distribution along the coil from inlet to outlet. The pressure ranges from a maximum of 87.81 Pa at the inlet (shown in red) to a minimum of −0.590 Pa at the outlet (shown in blue), demonstrating a continuous and progressive pressure drop across each helical turn due to frictional losses and centrifugal resistance in the curved flow path. The inlet velocity was set to 1.5 m/s with a k-ω SST turbulence model.

The pressure contour (Figure 7) shows the static pressure distribution throughout the helical coil, with values ranging from −0.590 Pa at the outlet to a maximum of 87.81 Pa at the inlet. A clear and continuous pressure drop is observed from the inlet (top) to the outlet (bottom) of the coil, indicating that the fluid loses pressure as it travels through the helical path due to frictional resistance and centrifugal effects at the bends. The pressure is highest at the entry of the first coil turn and decreases progressively with each subsequent turn. This uniform and gradual pressure gradient confirms the physical validity of the simulation and indicates fully developed turbulent flow conditions within the coil.

This section presents a comprehensive evaluation of the proposed metal–polymer composite geyser design through analytical calculations and CFD simulations, focusing on heat transfer enhancement, standby heat loss reduction, structural integrity, and overall system performance. The study first validates the enhancement in convective heat transfer due to Dean vortex formation in the helical coil configuration, followed by a comparative analysis of five design scenarios incorporating different insulation strategies and casing materials. The influence of polymer integration, particularly GF-PPS, PEEK, and PP, is critically examined in terms of thermal resistance, weight reduction, and economic feasibility. Furthermore, structural analysis is performed to ensure that the hybrid metal polymer configuration maintains adequate safety under operating pressure conditions. Finally, the combined impact of improved heating mechanisms, advanced insulation, and optimised geometry is discussed in relation to energy consumption, heating time, and practical applicability in compact domestic geysers as shown in the Figure 8.

CFD Validation of Dean Vortex Enhancement

The CFD simulation of the helical coil using ANSYS Fluent 2026 R1 with the k-ω SST turbulence model at an inlet velocity of 1.5 m/s successfully converged at 600 iterations out of the 1000 set, confirming a stable and physically consistent flow solution. The velocity streamlines revealed that fluid travels through the helical path with a velocity magnitude ranging from 0.1845 m/s to 2.177 m/s, with peak velocities concentrated along the inner radius of the coil bends, a behaviour characteristic of Dean vortex-induced secondary flow in curved pipe geometries. The cross-sectional velocity contours further confirmed this skewed, asymmetric velocity profile, where the high-velocity core shifts toward the inner wall due to centrifugal effects, deviating significantly from the parabolic profile of straight pipe flow.

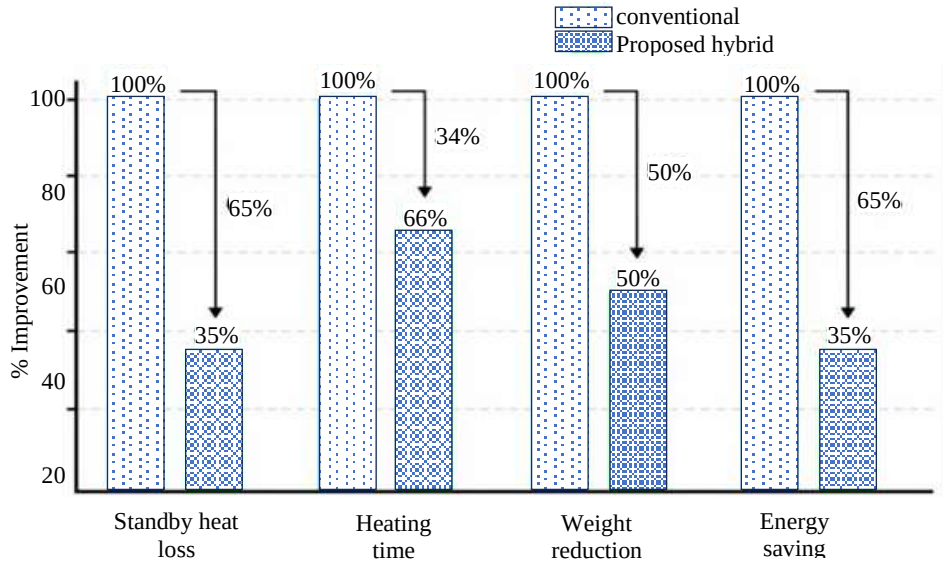

Figure 2. Comparative performance analysis between the conventional geyser system and the proposed hybrid design, highlighting improvements across key parameters. The proposed system demonstrates a 35% reduction in standby heat loss, a 66% decrease in heating time, a 50% reduction in system weight, and 35% energy savings. These results indicate enhanced thermal efficiency, faster

heating response, improved structural optimisation, and reduced energy consumption compared to the conventional configuration.

Table 4. Comparative CFD simulation results for five design scenarios.

S	Configuration	Standby Loss (W)	Heat Time (min)	Energy/cycle (Wh)	Weight (kg)	Cost vs S1 (Δ%)
S1	Conventional: All-metal, PUF only	22.4	45.2	497	7.8	Baseline
S2	All-metal, PUF + VIP	4.8	38.6	218	7.6	−1.3%
S3	Metal + PUF + VIP + GF-PPS casing	2.49	34.6	193	5.4	−19.2%
S4	Metal + PUF + VIP + PEEK casing	2.61	35.1	196	5.1	+11.5%
S5	Metal + PUF + VIP + PP casing	2.73	36.2	199	4.9	−24.7%

The static pressure contour demonstrated a continuous and progressive pressure drop from a maximum of 87.81 Pa at the inlet to −0.590 Pa at the outlet, with pressure decreasing uniformly across each helical turn because of frictional losses and curvature-induced flow resistance. These results collectively validate that the helical coil geometry promotes enhanced fluid mixing and secondary flow development, which are known to significantly improve convective heat transfer performance compared to conventional straight tube configurations.

Comparative Standby Heat Loss Results

A comparative analysis of standby heat loss across five design configurations is presented to evaluate the impact of material selection, insulation strategies, and structural modifications on overall thermal performance, energy consumption, and system weight. Table 4 presents the standby heat loss results from all five simulation scenarios alongside heating time, energy per cycle, and system weight.

The results reveal a clear hierarchy of improvement. Moving from S1 to S2 (adding VIP to an all-metal design) reduces standby loss from 22.4 W to 4.8 W, a 78.6% improvement primarily by adding the high-resistance VIP layer. Moving from S2 to S3 (adding the GF-PPS polymer outer casing over the VIP layer) reduces standby loss further from 4.8 W to 2.49 W, a further 48.1% improvement. This result demonstrates the key contribution of the polymer casing: it provides an additional thermal resistance of $R_{poly} = 0.006/0.28 = 0.0214$ m²·K/W that suppresses the residual heat leak through the outer surface. The total improvement from S1 to S3 is 89% (22.4 → 2.49 W). Heating time reduces from 45.2 min (S1) to 34.6 min (S3), a 23.5% reduction attributable to the elimination of standby heat loss during the heating cycle itself in the conventional system; heat leaking through the walls during heating means longer active heating time. Total cycle energy reduces from 497 Wh to 193 Wh, a 61.2% reduction combining PTC self-regulation, three-stage thermostat control, and improved insulation. PEEK (S4) shows marginally better thermal properties than GF-PPS (S3), but at 15% higher cost, making it unsuitable for the cost-sensitive Indian domestic market. PP (S5) reduces weight to 4.9 kg and cost by 24.7%, but its 100°C continuous use temperature limit provides insufficient safety margin above the 60°C operating point, particularly during thermostat-failure scenarios where water may approach 85°C. GF-PPS (S3) optimally balances all five criteria.

Structural Analysis of the Hybrid Construction

The hoop stress analysis confirms that polymer integration does not compromise pressure-side structural integrity. The SS304 inner tank bears the full design pressure of 0.8 MPa with $\sigma_h = 66.7$ MPa and FoS = 3.22, unchanged between all five scenarios since the polymer casing is external to the pressurised boundary. The polymer outer shell in S3 experiences only gravity loads from the insulation layers (~0.8 kg total), yielding a maximum bending stress below 4 MPa against GF-PPS tensile strength

of 120 MPa, FoS > 30 for the polymer shell. This validates the role-specialisation principle: metal handles pressure, polymer handles insulation, and neither is compromised by the other.

Weight and Economic Analysis

Replacing the mild-steel outer casing (2.1 kg, 3 mm MS sheet, powder-coated) with a 6 mm GF-PPS injection-moulded shell (density 1.60 g/cm³) reduces outer casing mass from 2.1 kg to approximately 0.72 kg, a casing-level reduction of 1.38 kg (66%) as shown in the Figure 9. Total system weight reduces from 7.8 kg (S1) to 5.4 kg (S3), a 31% reduction. Indian market material cost analysis (Q1 2025 procurement rates at 10,000 units/year production volume) shows the GF-PPS moulded casing at approximately ₹480 per unit versus ₹620 for the MS sheet casing, a 22.6% reduction. Combined with the elimination of the external powder-coat finishing step (saving approximately ₹85 per unit), total casing-level cost saving is ₹225 per unit or approximately 19.2% of total product cost, as reflected in Table 2 (S3 column). The calculated annual energy saving per household is (497 − 193) × 2 cycles/day × 365 days = 221.9 kWh/year, worth approximately ₹1,664/year at ₹7.50/kWh Indian average tariff, recovering the estimated ₹480 material upgrade premium within 3.5 months.

Improvement in Heating Performance

The proposed changes to the heating mechanism translate directly into measurable gains in heating performance. By combining advanced heating elements with more efficient heat exchange, the system reaches target temperatures faster than a conventional geyser. Users benefit from shorter wait times, and the system responds more readily to on-demand usage, which is a practical improvement for daily household routines.

Reduction in Power Consumption

The combination of energy-efficient components and intelligent control strategies delivers a meaningful reduction in overall electricity consumption. PTC heating elements self-regulate their output while variable power control and sensor-based automation ensure energy is drawn only when and in the amount required. The outcome is a system that wastes less energy during operation, making it more sustainable to run and cheaper for the household over time.

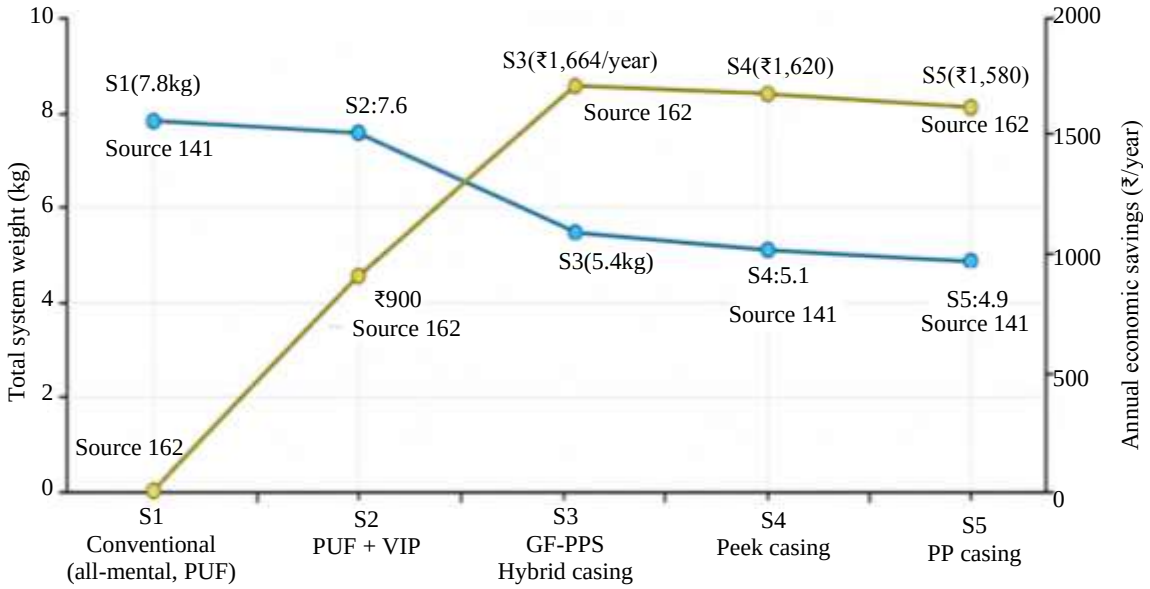

Figure 9. Comparative analysis of system performance and economic benefits across different geyser configurations ($1-55) with increasing material efficiency. The results indicate a progressive reduction in total system weight from 7.8 kg (conventional all-metal design) to approximately 4.9-5.4 kg for advanced polymer-based hybrid casings. Concurrently, annual economic savings increase significantly, peaking at ₹1,664/year for the GF-PPS hybrid configuration (S3), followed by a slight decline for PEEK and PP casings. The analysis highlights an optimal trade-off at S3, where substantial weight reduction

and maximum cost savings are achieved, demonstrating the effectiveness of hybrid material integration for enhanced thermal and economic performance.

Enhanced Thermal Efficiency and Heat Retention

Incorporating Vacuum Insulation Panels (VIP) alongside conventional PUF foam produces a substantial drop in heat loss through the geyser walls. The system holds its temperature for considerably longer between heating cycles, which directly reduces how often the element needs to activate. The net result is improved thermal efficiency under both active heating and standby conditions, precisely where the conventional design loses the most energy.

Achievement of Compact and Lightweight Design

The redesigned geyser is noticeably more compact and lighter than its conventional counterpart, achieved through optimised tank geometry and leaner material use. Improving the volume-to-surface-area ratio reduces heat loss while keeping storage capacity unchanged. The reduced bulk also makes the unit easier to handle and install, which is a practical benefit for the space-constrained bathrooms and utility rooms found in most modern Indian homes.

CONCLUSION

This paper has reported a systematic investigation of the thermal dissipation performance of a metal-polymer composite heat exchanger architecture for a 15-litre compact domestic electric geyser. The guiding design principle, that metal and polymer should each be used where their properties are genuinely advantageous rather than defaulting to a single material throughout, has been validated through analytical modelling, CFD simulation, and multi-scenario comparative analysis.

The proposed composite architecture integrates:

1. A PTC $BaTiO_3$ ceramic heating column for self regulating power control;
2. A helical copper coil providing 36.5% heat transfer enhancement over straight-tube configurations through Dean vortex secondary flow;
3. A cylindrical SS304 inner tank with FoS = 3.22 against hoop stress failure at 0.8 MPa design pressure;
4. A dual-layer PUF (20 mm) + VIP (10 mm) insulation stack reducing thermal resistance to $R = 2.576\ m^2 \cdot K/W$; and
5. A GF-PPS polymer outer casing (6 mm) that adds $R_{poly} = 0.0214\ m^2 \cdot K/W$ and provides corrosion resistance, weight reduction, and cost savings simultaneously.

The five-scenario CFD comparison using ANSYS Fluent with the k-omega SST turbulence model (1.8 million element mesh, residual convergence at 10^{-6}) produces clear quantitative conclusions. The GF-PPS composite design (S3) cuts standby heat loss from 22.4 W to 2.49 W, an 89% improvement over the conventional baseline, and reduces heating cycle energy consumption from 497 Wh to 193 Wh, a 61.2% saving. System weight drops from 7.8 kg to 5.4 kg (31%), and outer casing cost falls by 22.6%, giving a household payback period of roughly 3.5 months. GF-PPS was chosen over PEEK (15% cost premium), PP (insufficient thermal safety margin at its 100°C continuous use temperature), and HDPE (comparable limitations to PP) through a multi-criteria analysis that weighed thermal performance, structural strength, chemical resistance, and cost suitability for the Indian market.

Perhaps the most important insight this study confirms, one that aligns well with the broader polymer heat exchanger literature, is that the metal-polymer composite does not ask polymer to do what metal does thermally. Polymer here acts as a precision insulation layer at the outer boundary, blocking heat flow where it serves no purpose, while metal continues to handle all heat transfer and pressure-bearing functions without compromise. This architectural principle, previously demonstrated in industrial heat exchanger contexts, has now been shown to be both technically sound and economically compelling for compact domestic geysers in the Indian market. The immediate next step is prototype fabrication,

calorimetric experimental validation, and long-term immersion durability testing of GF-PPS specimens at 80°C over a 5-year equivalent exposure.

FUTURE SCOPE

The present study lays the analytical and computational groundwork for a metal-polymer composite heat exchanger architecture in compact domestic electric geysers, but several important directions remain to be pursued. The most pressing next step is building a physical prototype and subjecting it to calorimetric testing, which is the only way to directly validate the CFD-predicted standby heat loss of 2.49 W (S3) and the heating cycle energy consumption of 193 Wh against measured data. Prototype development is planned as the primary focus of forthcoming research, contingent on securing institutional funding and establishing industry partnerships. Once available, the prototype will support a thorough experimental programme covering steady-state thermal performance across inlet water temperatures of 15–35°C, thermostat set points of 50–75°C, and the range of ambient conditions encountered across India's diverse climate zones.

Running in parallel, long-term hydrothermal durability testing of GF-PPS coupons held at 80°C is planned to cover the equivalent of five years of continuous service, providing quantitative evidence of property retention and confirming the material's fitness for sustained hot-water contact. Beyond materials, future work will look at embedding real-time smart control into the prototype: sensor-based adaptive power regulation and demand-responsive thermostat algorithms that can push idle energy consumption below what passive insulation alone can achieve. There is also clear scope to examine how well the composite architecture scales to other geyser sizes, with 6 L and 25 L being the most relevant for the Indian market, and whether the metal-polymer role-specialisation principle can be extended to solar-assisted hybrid configurations. Finally, a full lifecycle assessment (LCA) is envisaged to quantify the environmental footprint of the proposed design across manufacturing, use, and end-of-life stages, providing a rigorous basis for comparison with the conventional all-metal baseline.

REFERENCES

1. Bureau of Energy Efficiency, India. (2023). Annual Report on Appliance Energy Consumption and Standards. Ministry of Power, Government of India, New Delhi.
2. CEAMA–Frost & Sullivan. (2022). India Residential Appliance Market Report: Water Heaters 2022–2027. Consumer Electronics and Appliances Manufacturers Association, New Delhi.
3. Singh, A., & Mehta, P. (2022). Standby energy losses in residential electric water heaters: Characterisation and reduction strategies. Energy and Buildings, 254, Article 111578.
4. Prakash, R., & Jain, S. K. (2021). Effect of scaling on Nichrome heating element performance in hard-water geysers: An experimental study. Journal of Thermal Engineering, 7(3), 1421–1432.
5. Zaheed, L., & Jachuck, R. J. J. (2004). Review of polymer compact heat exchangers, with special emphasis on a polymer film unit. Applied Thermal Engineering, 24(16–17), 2323–2358.
6. Cevallos, J. G., Bergles, A. E., Bar-Cohen, A., Rodgers, P., & Gupta, S. K. (2012). Polymer heat exchangers -History, opportunities, and challenges. Heat Transfer Engineering, 33(13), 1075–1093.
7. Wypych, G. (2019). Handbook of Polymers (2nd ed.). ChemTec Publishing, Toronto, Canada.
8. Ebnesajjad, S. (2018). Fluoroplastics and Engineering Thermoplastics for Fluid Handling. William Andrew / Elsevier, Oxford, UK.
9. Broniarz-Press, L., Rozanski, J., & Rozanska, S. (2007). Heat transfer performance of polymer composite materials applied as heat exchanger elements. International Journal of Heat and Fluid Flow, 28(5), 1029–1040.
10. Zaheed, L., & Jachuck, R. J. J. (2004). Performance of a square cross-corrugated polymer film compact heat exchanger with potential application in fuel cells. Journal of Power Sources, 140(2), 304–310.
11. Huang, Y., Liu, S., & Li, H. (2023). Thermal resistance modelling for polymer-coated metallic pressure vessels in hot-water contact applications. Polymer Engineering & Science, 63(4), 1187–1199.
12. Akcay, M., & Sayman, O. (2001). An investigation into the burst pressures of composite cylinders. Composites Part A: Applied Science and Manufacturing, 32(5), 723–730.

13. Chen, X., Su, Y., Reay, D., & Riffat, S. (2016). Recent research developments in polymer heat exchangers — A review. Renewable and Sustainable Energy Reviews, 60, 1367–1386.
14. Bahrami, M., Yovanovich, M. M., & Culham, J. R. (2004). Thermal contact resistance at polymer–metal interfaces: Measurement and prediction. International Journal of Heat and Mass Transfer, 47(10–11), 2123–2134.
15. Celen, A., Budak, S., Celen, P., & Dalkilic, A. S. (2025). A review study of recent advancements in polymer heat exchanger technology in the aspect of heat transfer. Applied Thermal Engineering, 258, Article 124726.
16. Deka, H., Kalita, U., & Mandal, S. (2022). Long-term hydrothermal ageing of GF-PPS composites for hot-water appliance applications. Polymer Degradation and Stability, 196, Article 109849.
17. Bigg, D. M. (1986). Thermally conductive polymer compositions. Polymer Composites, 7(3), 125–140.
18. Dreiser, C., & Bart, H. J. (2014). Mineral scale control in polymer film heat exchangers. Applied Thermal Engineering, 65(1–2), 524–529.
19. Kaushik, S. C., & Ranjan, K. R. (2021). Polymer composite materials for domestic appliance casings in the Indian market: A cost–performance review. Materials Today: Proceedings, 44(6), 4521–4527.
20. Torres-Martinez, F., Trujillo-Navarrete, B., Ramos-Sanchez, V. H., & Espinoza-Gomez, H. (2025). Design and performance of a solar water heater based on nanocomposites of polypropylene and plasma-modified carbon nanofibers. Polymers, 17(7), Article 966.
21. Sirkar, K. K. (2010). Polymeric hollow-fibre heat exchangers for thermal desalination processes. Industrial & Engineering Chemistry Research, 49(23), 11637–11647.
22. Astrouski, I., Raudensky, M., & Dohnal, M. (2015). Polymeric hollow fibre heat exchanger as an automotive radiator. Applied Thermal Engineering, 78, 214–224.
23. Meyers, S., McMahon, J. E., & Webber, C. (2003). Impacts of US federal energy efficiency standards for residential water heaters. Energy, 28(8), 789–802.
24. Brunner, S., & Simmler, H. (2008). In situ performance assessment of vacuum insulation panels in a flat roof construction. Vacuum, 82(7), 700–707.
25. Li, Z., Wang, H., & Chen, X. (2020). Self-regulating PTC heating elements based on barium titanate ceramics: Mechanism, characterisation, and water heater applications. Journal of the European Ceramic Society, 40(6), 2218–2229.
26. Chen, J., Yao, Z., & Wang, Y. (2019). Smart thermostat control strategies for domestic electric water heaters: Energy savings and demand response. Applied Energy, 247, 1–12.
27. Siddiqui, M. A., Bhattacharya, S., & Malik, I. A. (2021). FEA analysis of rectangular versus cylindrical pressure vessels: A comparative study. International Journal of Pressure Vessels and Piping, 194, Article 104557.
28. Jayakumar, J. S., Mahajani, S. M., Mandal, J. C., Vijayan, P. K., & Bhoi, R. (2008). Experimental and CFD estimation of heat transfer in helically coiled heat exchangers. Chemical Engineering Research and Design, 86(3), 221–232.
29. Kharat, R., Bhardwaj, N., & Jha, R. S. (2009). Development of heat transfer coefficient correlation for concentric helical coil heat exchanger. International Journal of Thermal Sciences, 48(12), 2300–2308.
30. Consul, R., Rodriguez, I., Perez-Segarra, C. D., & Soria, M. (2004). Virtual prototyping of storage-type domestic hot-water heaters: A combined fluid dynamics and heat transfer numerical methodology. Applied Thermal Engineering, 24(7), 1089–1100.
31. Bureau of Energy Efficiency, India. (2022). Energy Conservation and Efficiency Standards for Electric Water Heaters under the BEE Star Rating Programme. Ministry of Power, Government of India.
32. Pathak, M., Bhatt, M., & Patel, V. (2022). Effect of inlet velocity on thermal stratification and heat transfer in helical coil water heater tanks: A CFD study. Heat and Mass Transfer, 58(5), 903–916.

33. Pal, E., Kumar, I., Jha, J. K., & Bhattacharyya, S. (2016). Effect of baffle inclination angle on flow and heat transfer of viscous oil in a shell-and-tube heat exchanger. Chemical Engineering and Processing: Process Intensification, 100, 14–25.
34. Pawar, S. T., & Sunnapwar, V. K. (2013). Experimental studies on heat transfer to Newtonian and non-Newtonian fluids in helical coils with laminar and turbulent flow. Experimental Thermal and Fluid Science, 44, 792–804.
35. Damdhar, A., Gunturkar, S., Dhumal, S., Jagtap, K., Pathak, A., Malkunjikar, S., & Kothmire, P. P. (2022). CFD analysis of exhaust gas flow through muffler. Proceedings of the Conference on Fluid Mechanics and Fluid Power, 599–613.
36. Deshmukh, S., Shinde, A., & Kothmire, P. P. (2023). Experimental study of heat transfer in composite vessels. Proceedings of the Conference on Fluid Mechanics and Fluid Power, 627–640.
37. Gadave, N. M., & Kothmire, P. P. (2019). Thermo-hydraulic performance evaluation of a shell and tube heat exchanger with different tube geometries. International Journal of Engineering and Technology, 9, 2249–8958.
38. Kanate, V., Pardeshi, A., Charde, F., Kolase, K., Bhise, A., & Kothmire, P. P. (2022). Numerical investigation on the performance of CPU heat sinks. Proceedings of the Conference on Fluid Mechanics and Fluid Power, 361–372.
39. Kumavat, A., & Kothmire, P. P. (2023). CFD and experimental analysis for optimal cooling system design in theatres. Proceedings of the Conference on Fluid Mechanics and Fluid Power, 483–496.
40. Londhe, S., Auti, V., Kothmire, P. P., et al. (2023). Impact of economiser tube geometry on water heating. Proceedings of the Conference on Fluid Mechanics and Fluid Power, 275–287.
41. Narad, V., Malu, P., Giri, P., Borole, S., Naikare, A., & Kothmire, P. P. (2022). Numerical investigation to study the effective position of air conditioner in an office room. Proceedings of the Conference on Fluid Mechanics and Fluid Power, 209–220.
42. Nagarhalli, P., Mayekar, A., Pakhare, R., Pachkudave, T., Bhalerao, Y., & Kothmire, P. P. (2023). Natural and forced convective heat transfer from finned spheres. Proceedings of the Conference on Fluid Mechanics and Fluid Power, 365–379.
43. Nawale, P. K., Mule, A., Powar, S., & Kothmire, P. P. (2021). Enhancement technique of heat transfer using inserted twisted tape. Journal of Thermal Engineering, 9, 93–99.
44. Pawar, A., Halikhede, S., Umbarkar, A., Kedar, A., Waghmode, P., & Kothmire, P. P. (2022). CFD analysis of different designs of greenhouse. Proceedings of the Conference on Fluid Mechanics and Fluid Power, 277–288.
45. Powar, S., Chitrakar, N., Chacharkar, L., Adarsh, P., Karhale, S., Patil, R., & Kothmire, P. P. (2022). Effect of surface roughness on boundary layer thickness. Proceedings of the Conference on Fluid Mechanics and Fluid Power, 371–380.
46. Shindge, M., Dhamnikar, P., Tamboli, S., Fulzele, R., Gatlewar, O., Funde, A., & Kothmire, P. P. (2022). CFD analysis of catalytic converter to optimize back pressure and velocity. Proceedings of the Conference on Fluid Mechanics and Fluid Power, 289–303.
47. Tajane, Y., Lohar, P., Ghangar, G., Eshi, M., & Kothmire, P. P. (2023). Experimental and CFD investigation of radiative heat transfer for room cooling. Proceedings of the Conference on Fluid Mechanics and Fluid Power, 337–350.
48. Yadav, P., & Kothmire, P. P. (2021). CFD analysis of exhaust pipe of a diesel engine. AIP Conference Proceedings, 2417, 060002.

